A hydrodynamic water quality model for propagation of pollutants in rivers

Giorgio Mannina and Gaspare Viviani

ABSTRACT

Numerical modelling can be a useful tool to assess a receiving water body's quality state. Indeed, the use of mathematical models in river water quality management has become a common practice to show the cause-effect relationship between emissions and water body quality and to design as well as assess the effectiveness of mitigation measures. In the present study, a hydrodynamic river water quality model is presented. The model consists of a quantity and a quality sub-model. The quantity sub-model is based on the Saint Venant equations. The solution of the Saint Venant equations is obtained by means of an explicit scheme based on space-time conservation. The method considers the unification of space and time and the enforcement of flux conservation in both space and time. On the other hand, the quality sub-model is based on the advection dispersion equation. Particularly, the principle of upstream weighting applied to finite difference methods is employed. This method enable us to reduce the numerical dispersion avoiding oscillation phenomena. The optimal weighting coefficient was calculated on the basis of the mesh Peclet number. Regarding the quality processes, the model takes into account the main physical/chemical processes; these are degradation of dissolved carbonaceous substances, ammonium oxidation, algal uptake and denitrification, dissolved oxygen balance, including depletion by degradation processes and supply by physical reaeration and photosynthetic production. To properly simulate the river water quality, four state variables were considered: DO, BOD, NH_4, and NO. The model was applied to the Savena River (Italy), which is the focus of a European-financed project for which quantity and quality data were gathered. A sensitivity analysis of the model output compared to the model input or parameters was carried out.

Key words | advection, dispersion, pollution propagation, receiving stream, unsteady flow

Giorgio Mannina (corresponding author)
Gaspare Viviani
Dipartimento di Ingegneria Idraulica ed Applicazioni Ambientali,
Università degli Studi di Palermo,
Viale delle Scienze,
90128 Palermo,
Italy
E-mail: *mannina@idra.unipa.it*

INTRODUCTION

River water quality models can be useful tools to measure the effectiveness of water quality management measures. In fact, application of mathematical models for that purpose dates back to the initial studies on the Ohio River conducted between 1914 and 1916. These investigations provided the basis of the classic mathematical modelling of dissolved oxygen (DO) (Streeter & Phelps 1975). This model incorporates two primary mechanisms governing the fate of DO in rivers receiving sewage, decomposing organic matter and atmospheric aeration/reaeration. Since then, models have been constantly refined and updated to meet new and emerging problems of surface water pollution, such as eutrophication, acute and chronic toxicity (Rauch *et al.* 1998). The transport of solutes in open water bodies mainly consisting of advection, mixing, exchanging with the hyporheic zone, and mass reduction/generation by physical, chemical and biological mechanisms, can greatly affect stream water quality (e.g. Fischer *et al.* 1979; Chanson 2004). Solute transport modelling is needed to predict the movement, fate and associated risk of

doi: 10.2166/wst.2010.285

Downloaded from https://iwaponline.com/wst/article-pdf/446323/288.pdf
by guest

potentially harmful substances in flowing water, especially for contaminants released from either point or non-point sources. Water quality models are often implemented in order to quantify the substance transformation and to investigate the impact that changed boundary conditions have on an aquatic system (Wagenschein & Rode 2008). Indeed, water quality models have been developed to simulate physical, chemical and biological processes in bodies of water. Predicting changes in the constituent concentrations can be helpful for an ecologically oriented urban drainage planning (Ristenpart & Wittenberg 1991). However, especially for small rivers, some problems hamper a straightforward application of the model due to data scarcity, lack of major investments because of their minor importance, and the large number of diverse inputs, especially if they flow through densely populated areas (Marsili-Libelli & Giusti 2008). These facts constitute the major complexities for applying water quality models, such as those provided by the US Environmental Protection Agency; QUAL2E (Brown & Barnwell 1987), QUAL2K (Chapra & Pellettier 2003), WASP6 (Wool *et al.* 2001), or the IWA River Quality Model No. 1 (Reichert *et al.* 2001) require more information regarding the river system than is often available. Further, although many quality models have been implemented and are currently available, they are generally only applicable to stationary hydraulic components. Indeed, especially for small rivers, the influence of short-term impacts (e.g. combining sewer overflows) increases and causes severe problems for a river's ecosystem. Hydrodynamic water quality models are necessary to simulate these shock loads. However, as far as the authors know, there have not been many studies undertaken on small rivers.

Bearing in mind the considerations discussed above, the paper presents a water quality model to describe the dynamics of carbon and nitrogen in small river basins together with a sensitivity analysis to identify the most sensitive model parameters. Particularly, the model consists of a quantity and a quality sub-model. The quantity sub-model is based on the Saint Venant equations and the quality sub-model it is based on the advection dispersion equation. The model was applied to the Savena River (Italy), which was the focus of a European-financed project in which quantity and quality data were gathered.

THE HYDRODYNAMIC WATER QUALITY MODEL

The hydrodynamic water quality model is made up of two sub-models that are integrated to assess the propagation of pollutants in a river. The two model approach is inspired by Molls & Molls (1998) for the quantity sub-model and Wang & Lacroix (1997) for the quality sub-model. The mathematical formulation of the two sub-models is provided as follows, along with a brief description of the theory that goes beyond the model equations.

The quantity sub-model

The quantity sub-model is based on the resolution of the Saint Venant equations. Particularly, the conservative mass and momentum equations for 1D flow in an open channel can be written as follows:

$$\frac{\partial Q}{\partial t}+\frac{\partial (Q^2/A)}{\partial x}+g\cdot\frac{\partial I}{\partial x}=g\cdot A\cdot(i-j) \tag{1}$$

$$\frac{\partial A}{\partial t}+\frac{\partial Q}{\partial x}=0 \tag{2}$$

where Q is the discharge, t is the time, A is the wetted cross-sectional area, x is the longitudinal channel direction, g is the gravitational constant, I is the hydrostatic pressure force term, i is the channel slope and J is the friction slope. Equation (1) and (2) may be written in matrix form as follows:

$$\frac{\partial \bar{U}}{\partial t}+\frac{\partial \bar{G}}{\partial x}=\bar{S} \tag{3}$$

where:

$$\bar{U}=\left(\frac{A}{Q}\right);\quad \bar{G}=\left(\frac{Q}{Q^2/A+gI}\right);\quad \bar{S}=\left(\frac{0}{gA(i-J)}\right) \tag{4}$$

The numerical scheme

Using Green's theorem it is possible to demonstrate that Equation (3) represents the differential form of the integral conservation law:

$$\iint_A\left(\frac{\partial \bar{U}}{\partial t}+\frac{\partial \bar{G}}{\partial x}\right)\cdot dA=\oint_{S(A)}-\bar{G}\cdot dt+\bar{U}\cdot dx=\oint_{S(A)}\bar{f}\cdot dS=0 \tag{5}$$

Downloaded from https://iwaponline.com/wst/article-pdf/446323/288.pdf
by guest

where $\bar{f}=(\bar{G},\bar{U})$ is a 2D space-time vector. It should be noted that $\bar{f}$ ds represents the space-time flux of $\bar{f}$ leaving region A through ds. This leads to the unification of space and time and the enforcement of flux conservation in both space and time. The unification of the time and space is kept in the employed numerical method and represents one of the most important peculiarities of the technique. Once the mesh is defined, it is possible to consider a solution element (SE) around each mesh point. The space-time grid can be divided into non-overlapping rectangular regions called conservation elements (CE) (Figure 1).

Applying the conservation law reported above (Equation (5)) to the single CE elements and around the mesh point P yields the following expressions:

$$F\pm_{i,n} = \oint_{S(\mathrm{CE}\pm i,n)} \bar{f}\cdot \mathrm{d}s = 0 \tag{6}$$

where S(CE) is the boundary associated with a corresponding CE. From Equation (6), it is evident that the flux leaving the boundary of any CE is zero. Substituting the bidimensional vector f for its components yields:

$$F\pm_{i,n} = \oint_{S(\mathrm{CE}\pm i,n)} -\bar{G}\cdot \mathrm{d}t + \bar{U}\cdot \mathrm{d}x = 0 \tag{7}$$

where $\bar{G}(x,t)$ and $\bar{U}(x,t)$ are approximated by means of a first-order Taylor series in space and time. For every $(x,t)\in \mathrm{SE}(i,n)$ the approximations are:

$$\bar{U}^* = (\bar{U})_i^n + (\bar{U}_x)_i^n(x-x_i) + (\bar{U}_t)(t-t^n) + O(\Delta x^2, \Delta t^2) \tag{8}$$

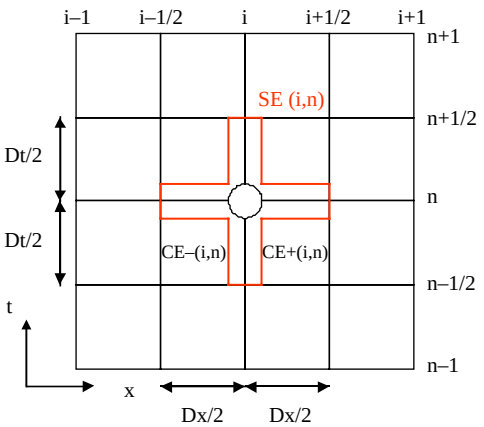

Figure 1 | Schematisation of the solution element SE (red) and of the conservative elements CE − and CE + (in black) of the mesh point P (i, n).

$$\bar{G}^* = (\bar{G})_i^n + (\bar{G}_x)_i^n(x-x_i) + (\bar{G}_t)(t-t^n) + O(\Delta x^2, \Delta t^2) \tag{9}$$

Because $\bar{f}=(\bar{G},\bar{U})$, it is possible to approximate this as $\bar{f}^*=(\bar{G}^*,\bar{U}^*)$ and to assume that each mesh element satisfies the governing equations:

$$\frac{\partial \bar{U}^*}{\partial t} + \frac{\partial \bar{G}^*}{\partial x} = 0 \tag{10}$$

Therefore, Equation (7) can be rewritten as follows:

$$F\pm_{i,n} = \oint_{S(\mathrm{CE}\pm i,n)} -\bar{G}^*\cdot \mathrm{d}t + \bar{U}^*\cdot \mathrm{d}x = 0 \tag{11}$$

Integrating Equation (11) across the SEs that represent the bound of each CE, from Figure 1 it is worthwhile to notice that the bound of each CE is constituted by the union of the two nearest SEs. It is possible to integrate the two equations as follows:

$$\frac{2}{\Delta x}\bar{F}+ = (\bar{U})_i^n + \frac{\Delta x}{4}(\bar{U}_x)_i^n - \frac{\Delta t}{\Delta x}(\bar{G})_i^n + \frac{\Delta t^2}{4\cdot\Delta x}(\bar{G}_t)_i^n - (\bar{U})_{i+1/2}^{n-1/2} - (\bar{W})_{i+1/2}^{n-1/2} \tag{12}$$

$$\frac{2}{\Delta x}\bar{F}- = (\bar{U})_i^n - \frac{\Delta x}{4}(\bar{U}_x)_i^n + \frac{\Delta t}{\Delta x}(\bar{G})_i^n - \frac{\Delta t^2}{4\cdot\Delta x}(\bar{G}_t)_i^n - (\bar{U})_{i+1/2}^{n-1/2} + (\bar{W})_{i+1/2}^{n-1/2} \tag{13}$$

where:

$$(\bar{W})_{i\pm1/2}^{n-1/2} = \frac{\Delta x}{4}(\bar{U}_x)_{i\pm1/2}^{n-1/2} + \frac{\Delta t}{\Delta x}(\bar{G})_{i\pm1/2}^{n-1/2} + \frac{\Delta t^2}{4\cdot\Delta x}(\bar{G}_t)_{i\pm1/2}^{n-1/2} \tag{14}$$

$$(\bar{G}_t) = -\left(\frac{\partial \bar{G}}{\partial \bar{U}}\right)^2 \frac{\partial \bar{U}}{\partial x} = -J^2(\bar{U}_x) \tag{15}$$

By rearranging Equations (14) and (15) considering the summation, the first part of the numerical scheme can be obtained:

$$(\bar{U})_i^n = \frac{1}{2}\left[(\bar{U})_{i-1/2}^{n-1/2} + (\bar{U})_{i+1/2}^{n-1/2} + (\bar{W})_{i-1/2}^{n-1/2} - (\bar{W})_{i+1/2}^{n-1/2}\right] \tag{16}$$

$$(\bar{U})_{i\pm1/2}^{n} = (\bar{U})_{i\pm1/2}^{n-1/2} + \frac{\Delta t}{2}(\bar{U}_t)_{i\pm1/2}^{n-1/2} \tag{17}$$

The second part of the numerical scheme can be obtained by evaluating the derivate of the flux vector $(\bar{U}_x)_i^n$ obtained extending $(\bar{U}_x)_{i\pm1/2}^{n-1/2}$ to $(\bar{U}_x)_{i\pm1/2}^{n}$ by means of

Downloaded from https://iwaponline.com/wst/article-pdf/446323/288.pdf
by guest

Taylor's series and taking the weighted average of forward and backward differences:

$$(\bar{U}_x)_i^n = \frac{\left|(\bar{U}_{x+})_i^n\right|^\omega (\bar{U}_{x-})_i^n + \left|(\bar{U}_{x-})_i^n\right|^\omega (\bar{U}_{x+})_i^n}{\left|(\bar{U}_{x+})_i^n\right|^\omega + \left|(\bar{U}_{x-})_i^n\right|^\omega} \tag{18}$$

where:

$$(\bar{U}_{x\pm})_i^n = \pm \frac{(\bar{U})_{i\pm1/2}^n - (\bar{U})_i^n}{\Delta x/2} \tag{19}$$

The weighted average of the derivates is controlled by a single parameter ω. If the parameter is $\omega = 0$, then the central difference is obtained; this is suitable for smooth regions. On the other hand, values higher than or equal to one or two are typical of the slope-limiters proposed by van Albada *et al.* (1982) and Molls & Molls (1998). The numerical scheme employs a staggered grid. At each grid point the flow variables, at a given time level, are calculated using the two neighbouring nodes from the previous time level. Figure 2 depicts a graphical representation of the method.

Let us denote $n - 1$ as the time step during which the overall values are known and with n being the time step when the values are unknown and with $n - 1/2$ as the intermediate time step, with i being the spatial localisation of the node, with $j - 1$ and $j + 1$ as the nodes at upstream and downstream, respectively, and with $i - 1/2$ and $i + 1/2$ as the intermediate values. The application of the numerical schemes is basically a stepwise procedure. Specifically, starting from the nodes at time step $n - 1$, we can calculate the values of the terms that represent vector $\bar{U}$ at time step $n - 1/2$ by employing Equation (16) (Figure 2(a)).

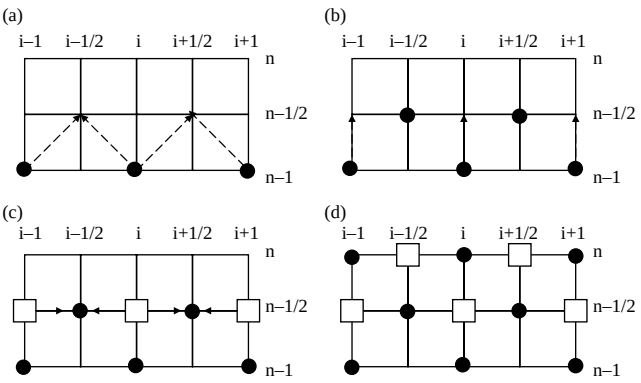

Figure 2 | Representation of the numerical scheme: (a) evaluation of unknown variables at intermediate time and space; (b) evaluation of the unknown variables at intermediate time and space at the nodes; (c) evaluation of the derivates of the variables at intermediate time and space; (d) conclusion of the numerical scheme.

Thereafter, we can calculate the unknown values at an intermediate time step at the nodes and using Equation (17) (Figure 2(b)). By means of Equation (18), we can calculate the derivates at an intermediate time step starting from the known values at the same time step and for the nodes indicated by squares (Figure 2(c)).

In Figure 2(d), a representation of a complete temporal loop has been depicted. The nodes are indicated by a circle. The unknown variables and their derivates have been calculated; on the other hand, at a point denoted by a square, only the variables are known. To allow the methods to converge, it is not necessary to consider any artificial viscosity.

The quality sub-model

The quality sub-model is based on the advection-dispersion equation whose solutions enable us to evaluate the pollutant propagation in the river. The general form of the advection-dispersion equation can be written as follows:

$$\frac{\partial C}{\partial t} + u \cdot \nabla C = \nabla \cdot (D \nabla C) + q \tag{20}$$

where t is the time, C is the concentration of a dilute solute, u is the velocity vector of fluid, D is the dispersion tensor and q is the source or sink term. Considering the case of a one dimensional transport with the hypothesis of a zero source or sink and a positive velocity, Equation (1) can be rewritten as:

$$\frac{\partial C}{\partial t} + u\frac{\partial C}{\partial x} = D_L \frac{\partial^2 C}{\partial x^2} + \frac{dC}{dt} \tag{21}$$

Using the finite difference algorithm, for a given constant spatial increment Δx and a time step Δt, Equation (21) may be rewritten in a general discretised form:

$$\frac{C_i^{n+1} - C_i^n}{\Delta t} + \{\bar{u}[\omega\Delta_x^- + (1 - \omega\Delta_x^+)] - D_L\Delta_{xx}\} \left[\vartheta C_i^{n+1} + (1 - \vartheta)C_i^n\right] = r \cdot C_i^{n+1} + P + \varepsilon_L \tag{22}$$

Downloaded from https://iwaponline.com/wst/article-pdf/446323/288.pdf
by guest

where ε_L is local error truncated by a finite difference approach, i and n are the spatial and time indices respectively, ϑ is the time weighting coefficient, ω is the spatial weighting coefficient, P is the internal constituent sources and sinks (e.g. nutrient loss from algal growth, benthos sources, etc.), r is the first order rate constant of a constituent and the mathematical operators are defined as in the following:

$$\left.\begin{aligned}\Delta_x^- C_i &= (C_i^n - C_{i-1}^n)/\Delta x\\ \Delta_x^+ C_i &= (C_{i+1}^n - C_i^n)/\Delta x\\ \Delta_{xx} C_i &= (C_{i+1}^n - 2C_i^n + C_{i-1}^n)/\Delta x^2\end{aligned}\right\} \tag{23}$$

In Figure 3, we present the orderly grid that is used to solve the advection dispersion equation. In Equation (23), n is the time and it must be set as the same as the corresponding multiplied concentration (i.e. $\Delta_x^- C_i \cdot C_i^n = (C_i^n - C_{i-1}^n)/\Delta x$).

Development of Equation (22) gives:

$$\frac{C_i^{n+1} - C_i^n}{\Delta t} + \left\{\begin{array}{c} u\left[\vartheta\omega\frac{(C_i^{n+1} - C_{i-1}^{n+1})}{\Delta x} + \vartheta(1-\omega)\frac{(C_{i+1}^{n+1} - C_i^{n+1})}{\Delta x}\right]^+ \\ -\vartheta D_L\frac{(C_{i-1}^{n+1} - 2C_i^{n+1} + C_{i+1}^{n+1})}{\Delta x^2}\end{array}\right\} + \left\{\begin{array}{c} u\left[(1-\vartheta)\omega\frac{(C_i^n - C_{1-1}^n)}{\Delta x} + (1-\vartheta)(1-\omega)\frac{(C_{i+1}^n - C_i^n)}{\Delta x}\right]^+ \\ -(1-\vartheta)D_L\frac{(C_{i-1}^n - 2C_i^n + C_{i+1}^n)}{\Delta x^2}\end{array}\right\} = r\cdot C_i^{n+1} + P + \varepsilon_L \tag{24}$$

Rearranging the terms and summing up the special term from Equation (24) reduces Equation (24) to:

$$\begin{aligned} &a\cdot C_{i-1}^{n+1} + b\cdot C_i^{n+1} + c\cdot C_{i+1}^{n+1} + d\cdot C_{i-1}^n + e\cdot C_i^n + f\cdot C_{i+1}^n \\ &\quad = \varepsilon_L\Delta t + P\cdot\Delta t \end{aligned} \tag{25}$$

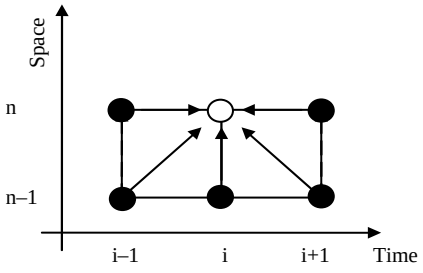

Figure 3 | Grid of the difference scheme.

where:

$$a = -\vartheta\left(u_{i-1}^{n+1}\omega\frac{\Delta t}{\Delta x} + D_L\frac{\Delta t}{\Delta x^2}\right) \tag{26}$$

$$b = \left[1 + \vartheta\left(u_i^{n+1}(2\omega - 1)\frac{\Delta t}{\Delta x} + D_L 2\frac{\Delta t}{\Delta x^2}\right) - r\cdot\Delta t\right] \tag{27}$$

$$c = \vartheta\left[u_{i+1}^{n+1}(1-\omega)\frac{\Delta t}{\Delta x} - D_L\frac{\Delta t}{\Delta x^2}\right] \tag{28}$$

$$d = (1-\vartheta)\left(-u_{i-1}^n\omega\frac{\Delta t}{\Delta x} - D_L\frac{\Delta t}{\Delta x^2}\right) \tag{29}$$

$$e = \left[-1 + (1-\vartheta)\left(u_i^n(2\omega - 1)\frac{\Delta t}{\Delta x} + D_L 2\frac{\Delta t}{\Delta x^2}\right)\right] \tag{30}$$

$$f = (1-\vartheta)\left(u_{i+1}^n(1-\omega)\frac{\Delta t}{\Delta x} - D_L\frac{\Delta t}{\Delta x^2}\right) \tag{31}$$

Applying Taylor's formula, the local truncated error can be expressed as (Wang & Lacroix 1987):

$$\varepsilon_L = u\cdot\Delta x\left[(\omega - 0.5) + \frac{u\cdot\Delta t}{\Delta x}(\vartheta - 0.5)\right]\frac{\partial^2 C}{\partial x^2} + O(\Delta t^2, \Delta x^2) \tag{32}$$

and, by neglecting the second-order term $O(\Delta t^2, \Delta x^2)$, Equation (32) becomes:

$$D_{\text{num}} = u\cdot\Delta x\left[(\omega - 0.5) + \frac{u\cdot\Delta t}{\Delta x}(\vartheta - 0.5)\right] \tag{33}$$

Substituting that gives:

$$\varepsilon_L = D_{\text{num}}\frac{\partial^2 C}{\partial x^2} \tag{34}$$

The term (Equation (34)) introduced by the finite difference approach is known as numerical dispersion.

Downloaded from https://iwaponline.com/wst/article-pdf/446323/288.pdf
by guest

The numerical dispersion can be cancelled by adopting appropriate values of ω,ϑ (e.g. $\omega = \vartheta = 0.5$). If $\omega = 0.5$, Equation (25) transforms into the well-known Crank-Nicolson scheme, which is unconditionally stable for $0.5 \leq \omega \leq 1$. Assuming $\omega = 1$, the method becomes a space-centred scheme without numerical dispersion. Therefore, Equation (34) becomes:

$$a \cdot C_{i-1}^{n+1} + b \cdot C_i^{n+1} + c \cdot C_{i+1}^{n+1} + d \cdot C_{i-1}^{n} + e \cdot C_i^{n} + f \cdot C_{i+1}^{n} = P \cdot \Delta t \quad (35)$$

After rearranging the Equations, we find:

$$a \cdot C_{i-1}^{n+1} + b \cdot C_i^{n+1} + c \cdot C_{i+1}^{n+1} = z_i \quad (36)$$

$$z_i = -d \cdot C_{i-1}^{n} - e \cdot C_i^{n} - f \cdot C_{i+1}^{n} + P \cdot \Delta t \quad (37)$$

The developed scheme has been tested considering analytical solutions aimed at verifying the absence of oscillation and numerical dispersion that generally limit the reliability of numerical solutions of the advection-dispersion equation when finite difference methods are employed. Such trials, not showed herein for sake of conciseness, confirmed the goodness of the approach that eliminates the oscillation and reduce the numerical dispersion thanks to upstream weighting coefficients. Nevertheless, it should be stressed that other numerical schemes could be employed such in the case of the quickest scheme of Leonard (1979) that generally reduce wiggles especially when numerical dispersion is being minimized. and the results confirmed.

Assessment of first order rate constants and internal constituents

In order to assess the aquatic ecosystem of the river, four state variables have been considered; these are DO, BOD, NH_4, and NO. The processes considered are degradation of dissolved carbonaceous substances, ammonium oxidation, algal uptake and denitrification, dissolved oxygen balance, including depletion by degradation processes and supply by physical reaeration and photosynthetic production (Figure 4). In particular, two DO sources were considered, namely, reaeration from the atmosphere and photosynthesis of algae and plants. However, DO is consumed via plant

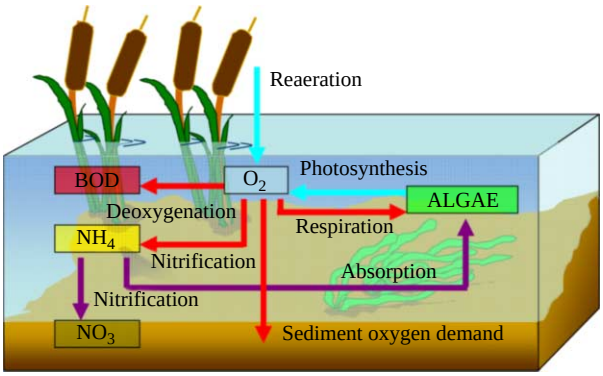

Figure 4 | Quality sub-module modelled processes.

respiration, nitrification processes, and BOD degradation. All processes are described assuming 1st order kinetics. The first order constants (r_i) and the internal constituent sources and sinks (P_i) employed in the model are derived according to previous studies (Thomann & Muller 1987; Chapra 1997; Marsili-Libelli & Giusti 2008):

$$r_{\mathrm{BOD}} = K_{D(20^\circ)} \cdot \vartheta_D^{(T-20)} \cdot \frac{\mathrm{BOD}}{K_{\mathrm{s\_BOD}} + \mathrm{BOD}} + K_{\mathrm{sed}} \quad (38)$$

$$r_{\mathrm{NO}} = K_{\mathrm{Den}} \cdot \vartheta_{\mathrm{Den}}^{(T-20)} \quad (39)$$

$$r_{\mathrm{NH_4}} = K_{\mathrm{N}(20^\circ)} \cdot \vartheta_N^{(T-20)} \cdot \frac{\mathrm{NH_4}}{K_{\mathrm{s\_NH_4}} + \mathrm{NH_4}} \quad (40)$$

$$r_{\mathrm{NO}} = k_{\mathrm{Den}} \cdot \vartheta_{\mathrm{Den}}^{(\mathrm{Temp}-20)} \quad (41)$$

$$r_{\mathrm{DO}} = k_R \quad (42)$$

$$P_{\mathrm{NH_4}} = -y_{\mathrm{resp}}(p_h - r_s) \quad (43)$$

$$P_{\mathrm{NO}} = +r_{\mathrm{NH_4}} \cdot \mathrm{NH}_{4\mathrm{i}}^{k+1} \quad (44)$$

$$P_{\mathrm{DO}} = r_{\mathrm{DO}} \cdot \mathrm{DO_{SAT}} - r_{\mathrm{BOD}} \cdot \mathrm{BOD} - r_{\mathrm{NH_4}} \mathrm{NH_4} - r_S \vartheta_{\mathrm{resp}}^{\mathrm{Temp}-20} + P_h \quad (45)$$

where K_{D} is the deoxygenation coefficient, ϑ_D is the Arrhenius temperature coefficient of the degradation process, T is the temperature, K_{sed} is sediment oxygen demand, and $K_{\mathrm{s\_BOD}}$ is the half saturation constant for the BOD, K_{N} is the nitrogen coefficient, K_{Den} is the denitrification coefficient, ϑ_N is the Arrhenius temperature coefficient of the nitrification process, $K_{\mathrm{s\_NH_4}}$ is the half saturation constant for ammonium, ϑ_{Den} is the Arrhenius temperature coefficient of the denitrification process, $\vartheta_{\mathrm{resp}}$ is the

Downloaded from https://iwaponline.com/wst/article-pdf/446323/288.pdf
by guest

Arrhenius temperature coefficient of the respiration processes, P_h is the actual production of oxygen due to photosynthesis and K_R is the reaeration constant.

THE CASE STUDY

The river studied in this work and the field data gathering campaign were part of an earlier European-financed project (Artina *et al.* 1998, 1999). A brief description of the system is reported herein, but more detailed information is available in previous studies (Artina *et al.* 1998, 1999). The Savena is a rural ephemeral river that passes through a number of small towns before entering the southern neighbourhood of Bologna (Figure 5). The catchment area of the Savena, at the downstream boundary of the studied river reach, is nearly 160 km^2. The river is characterised by a quite variable hydraulic regime with discharge usually ranging from a few litres per second during dry summer periods up to several cubic meters per second during wet weather. The studied river reach is about 6 km long, receiving six combined sewer overflow (CSO) discharges from the Bologna sewer network and twelve from the San Lazzaro sewer systems, a small centre in the surrounding area of Bologna. CSOs generally occur during low intensity rainfalls, and, in many cases, their discharge is similar to the river's discharge. The sewer network is a part of the combined system serving the whole city of Bologna, which can be treated as hydraulically divided into many independent catchments, all connected to a WWTP. The city of Bologna has about

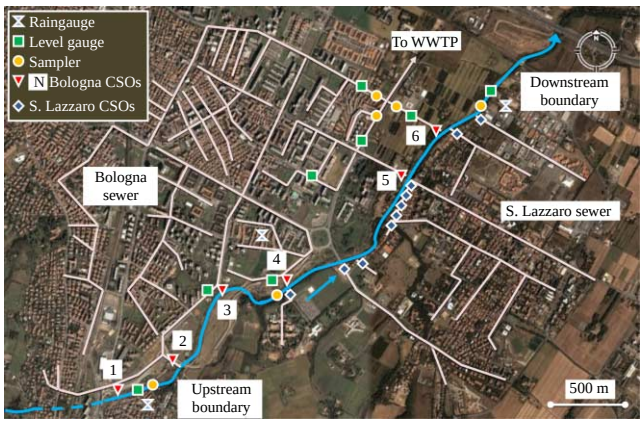

Figure 5 | Savena case study (Bologna—Italy).

500,000 inhabitants and an equivalent population of about 800,000 inhabitants. Only the part of this catchment, which has an effect on the studied reach of the Savena River, has been taken into account. This part of Bologna covers an area of more than 450 ha, with an impervious percentage of about 66% and about 60,000 inhabitants. About 50 events were recorded during an experimental survey from December 1997 to July 1999, but water quality aspects were analysed for both RWB and SS for only five of these. The analysed parameters were as follows: BOD_5, NH_4, TSS, COD, pH, DO, temperature, and conductivity. The considered events are characterised by small rainfall volumes with rapidly varying intensities. Those events are only partially representative of the climatic conditions in the Bologna area that are typically characterised by an high frequency of small events in winter and spring, by intense and short events in early autumn, and a long dry period between May and September. Nevertheless, those events are representative of the actual catchment situation in terms of polluting loads, that is, high frequency and small rainfall volume events activate CSOs. During the five monitored events, only one of the six CSOs discharged into the river (CSO No. 6), and, for this reason, results are presented only for the last trunk of Savena urban reach (400 m downstream of the CSO). Even if the analysed river reach is rather short, the measured data show that, especially during storm events, its ephemeral behaviour and significant turbulence associated with flood events guarantee sufficient depletion of polluting concentrations (Mannina & Viviani 2010). Because the analysed urban area is 5.7 km^2, which is equivalent to 3.2% of the total catchment surface, the contribution of the upstream polluting sources was determined by monitoring the pollution load in the first cross-section upstream of the urban area and using this information as inputs for the models.

MODEL CALIBRATION AND SENSITIVITY ANALYSIS

The model was applied considering the five events of the Savena case study separately. Because the database was limited, a model validation was not carried out. The calibration was done in two steps. In the first step, hydraulic parameters were evaluated considering measured flow

Downloaded from https://iwaponline.com/wst/article-pdf/446323/288.pdf
by guest

data. In the second step, quantity parameters were set to calibration values to assess quality parameters. The model calibration was carried out using Generalised Likelihood Uncertainty Estimation (GLUE) methodology (Beven & Binley 1992). GLUE is a Monte Carlo simulation approach developed as an attempt to recognise more explicitly the underlying uncertainties of models simulating environmental processes. The GLUE approach rejects the concept of an optimum parameter set and assumes that, prior to the input of data into a model, all parameter sets have an equal likelihood of being acceptable estimators of the system in question. Many parameter sets are generated from specified ranges using the Monte Carlo simulation. The performance of individual parameter sets is then assessed via likelihood measurements, which are used to weight the predictions of different parameter sets. This includes rejecting some parameter sets as non-behavioural. All other weights from behavioural or acceptable runs are retained and rescaled so that their cumulative total is equal to one. The cumulative likelihood weighted distribution of predictions can then be used to estimate quantiles for the predictions at any time step. The likelihood measure represents the ability of the model to fit actual data. The acceptability threshold Tr represents a user-defined critical value indicating the minimum value of the likelihood measure that each modelling simulation should have to represent model behaviour with respect to the goal of the analysis. Tr is usually set equal to zero. In the present study, the Nash and Sutcliffe efficiency index was used as the likelihood measure (Nash & Sutcliffe 1970):

$$E_j = 1 - \frac{\sum_{i=1}^{n} (O_i - P_i)^2}{\sum_{i=1}^{n} (O_i - \bar{O})^2} \quad (46)$$

where O is observation, P is model prediction, $\bar{O}$ is the mean value of model predictions and observations, respectively, and n is the number of observations. The subscript "j" indicates the state analysed variable (in this study, Q, BOD and DO were considered as model outputs). The model calibration and therefore the assessment of the model parameter set that provides the best fit between measured and simulated values were chosen in correspondence to the maximum value of the Nash and Sutcliffe efficiency index.

The GLUE can be also used to analyse the impact of each parameter on modelling outputs. Plotting the cumulative likelihood distributions for the set of behavioural simulations ($E \geq \mathrm{Tr}$) and the set of unconditioned cumulative distributions, respectively, it is possible, by comparing the deviation between the two, to determine if the model output in question is sensitive to changes in parameter values. If little difference between the two CDFs is found, the parameter is considered insensitive with regards to the model output, and, on the contrary, if a great difference is found, the parameter is considered to be sensitive. Applying the nonparametric Kolmogorov–Smirnov d-statistic (maximum distance between the two CDFs), a measure of sensitivity is introduced, i.e. $d = 1$ is the most sensitive and $d = 0$ is non-sensitive (Hornberger & Spear 1981; Beven *et al.* 2008; Freni *et al.* 2009). This sensitivity analysis is used to determine the relative importance of each parameter in the model structure. It is evident that the GLUE results can be affected by the definition of parameter variation ranges that can influence the analysis, because it defines the domain where the model uncertainty is evaluated. The selection of the parameter variation ranges can be accomplished by considering the physical meaning of the parameters, but this approach cannot be used for conceptual parameters that have a weak link to the physical system. In addition, this approach can produce variation intervals that are too wide, thereby leading to the problems described above. To avoid this source of subjectivity, the parameter variation ranges used in this study were estimated by calibration using multiple events (Beven & Binley 1992). Concerning the model calculation grid, for the present application, a Dx equal to 25 m and a dt equal to 1 s have been employed.

RESULTS

A Monte Carlo procedure was used to generate large numbers of sets of parameters for both sub-models thought feasible for the Savena River on the basis of physical argument and previous experience (Willems 2000; Cox 2003; Radwan *et al.* 2003; Marsili-Libelli & Giusti 2008; Mannina & Viviani 2010). In Table 1, the employed variation ranges for model parameters are provided.

Figure 6 shows the conditioned cumulative distributions (likelihoods) and the unconditioned cumulative

Downloaded from https://iwaponline.com/wst/article-pdf/446323/288.pdf
by guest

Table 1 | Variation ranges of model parameters

Parameter	Unit	Lower limit	Upper limit	References
River bed roughness (ks)	$m^{1/3} s^{-1}$	10	80	Willems (2000)
Longitudinal dispersion coefficient (D_L)	$m^2 s^{-1}$	0.01	20	Mannina (2005); Freni *et al.* (2009)
Reoxygenation constant (K_R)	s^{-1}	0.003	0.009	Marsili-Libelli & Giusti (2008)
Deoxygenation constant (K_D)	s^{-1}	0.001	0.008	Marsili-Libelli & Giusti (2008)
Actual Oxygen production (P_h)	$g O_2 l^{-1} s^{-1}$	0.02	0.05	Radwan *et al.* (2003); Mannina & Viviani (2010)
Respiration (r_s)	$g O_2 l^{-1} s^{-1}$	0.02	0.05	Radwan *et al.* (2003); Mannina & Viviani (2010)
Denitrification coefficient (K_{DEN})	d^{-1}	0.1	1	Radwan *et al.* (2003); Mannina & Viviani (2010)
Half saturation constant for the ammonium ($K_{s\_NH_4}$)	$mg N l^{-1}$	0.01	0.03	
Nitrogen coefficient (K_N)	d^{-1}	0.54	1.55	Cox (2003); Marsili-Libelli & Giusti (2008)
Sediment oxygen demand (K_{sed})	s^{-1}	0.001	0.01	Chapra (1997)
Half saturation constant (K_{s_BOD})	mg/l	0.001	0.1	Marsili-Libelli & Giusti (2008)

distributions based on Nash and Sutcliffe efficiency for some model parameters. In Table 2, the values of the Kolmogorov–Smirnov d-statistic for model parameters are reported. The results reveal that the most sensitive parameters are the ones connected to processes of dispersion and deoxigenation-reareation. More specifically, the Kolmogorov–Smirnov d-statistics of the longitudinal dispersion coefficient are 0.236 and 0.216 for BOD and DO, respectively (Table 2). The reaeration coefficient (K_R) shows a strong sensitivity for DO (Figure 6). Indeed, the Kolmogorov–Smirnov d-statistic showed a value of 0.225 (Table 2). On the other hand, the processes that are related to the oxygen contribution due to photosynthesis phenomena are less sensitive. These results are in agreement with the physics of the phenomenon. Indeed, during storm events, especially for an ephemeral river such as the Savena, the largest contribution of oxygen comes from the reaeration with the atmosphere due to the intense flow turbulence.

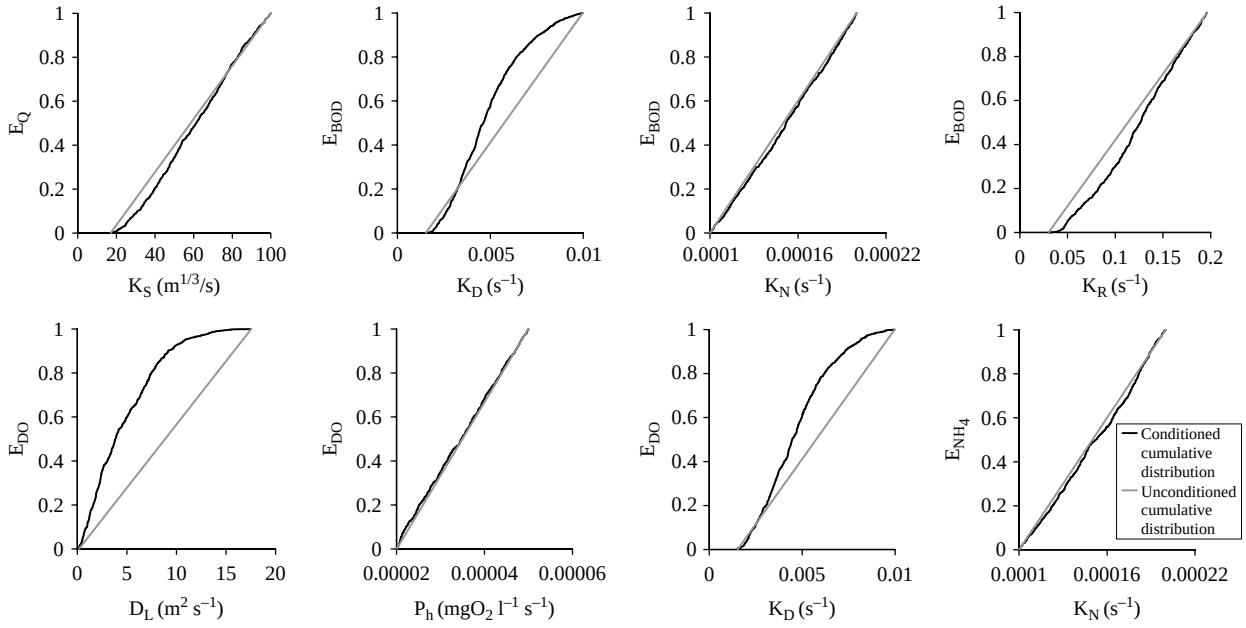

Figure 6 | Conditioned cumulative distributions and unconditioned cumulative distributions for some model parameters of the quantity and quality sub-models.

Downloaded from https://iwaponline.com/wst/article-pdf/446323/288.pdf
by guest

Table 2 | Kolmogorov-Smirnov d-statistic coefficients for model parameters and for different model outputs

	Model output			
Model parameters	***Q***	**BOD**	**DO**	**NH_4**
ks	0.102	0.0288	0.0225	0.0264
D_L	–	0.236	0.216	0.0943
K_R	–	0.224	0.225	0.0084
K_D	–	0.162	0.171	0.0923
P_h	–	0.0624	0.0632	0.1262
r_s	–	0.0233	0.0171	0.0514
K_{DEN}	–	0.0180	0.0087	0.143
$K_{s\_NH_4}$	–	0.0397	0.0151	0.0482
K_N	–	0.0172	0.0111	0.0970
K_{sed}	–	0.0132	0.0103	0.0151
K_{s_BOD}	–	0.0634	0.0505	0.081

This aspect is shown in terms of reaeration coefficient values. In particular, the latter values are some order of magnitude higher with respect to dry weather ones. This confirms the important role played by flow turbulence during stormy weather. The intense turbulence is obviously caused by the high increment of the river flow with respect to dry weather flow. Such an increment can be of some order of magnitude and it is due, especially for the ephemeral river, to the intermittent discharges coming from urban sewer systems, i.e. the CSOs.

Figure 7 shows a comparison between measured and simulated values. The model generally does an acceptable job of reproducing most of the observed data.

In terms of the Nash-Sutcliffe efficiency, the model is characterised by different values for the quantity and quality modules (Table 3). For example, the quantity module efficiency ranges from 0.632 to 0.923, while the quality module efficiency ranges from 0.172 to 0.872.

For quality variables, the modelling results were reasonable (Figure 7), although the measured values are slightly biased from simulated ones. Indeed, deviations occurred in the ammonia and oxygen values that can be attributed mainly to the higher complexity of phenomena involved with such variables. Indeed, ammonia and oxygen concentration values are the result of several chemical/

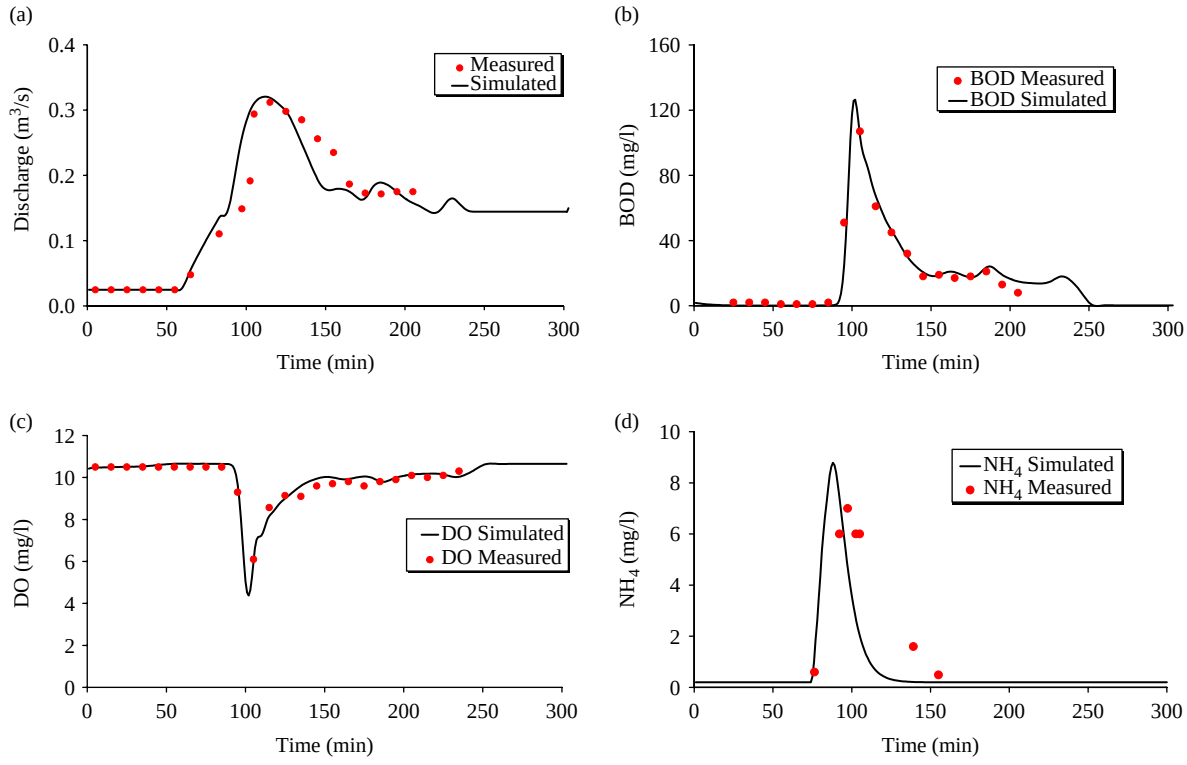

Figure 7 | Model results for the Savena river for the events of 22/5/98 for quantity [(a)] and for quality aspects [(b), (c) and (d)].

Downloaded from https://iwaponline.com/wst/article-pdf/446323/288.pdf
by guest

Table 3 | Nash-Sutcliffe efficiencies for the simulated events

Event	E_Q	E_{BOD}	E_{DO}	E_{NH_4}
22/5/98	0.632	0.810	0.872	0.056
28/5/98	0.827	0.733	–	0.429
28/11/98	0.717	0.419	0.597	0.531
27/1/99	0.881	0.703	0.365	–
22/3/99	0.923	0.347	–	–

physical/biological processes (i.e. nitrification, denitrification, photosynthesis, atmospheric reaeration, etc.). A slight miscalculation of these processes may contribute to high disagreement between measured and simulated values for ammonia and oxygen concentrations (Mannina & Viviani 2010).

For the event of 22/5/98, similarly to the other events, the flow rate in the RWB becomes more than an order of magnitude higher with respect to the dry weather event (Figure 7(a)). This causes the establishment of dynamic conditions in the RWB, and, hence, high turbulence conditions inside the water column. These phenomena play relevant roles with respect to water quality variables; the initial peak is mainly due to advective characteristics of the flow, and the polluting load discharge by the urban areas is diluted and rapidly transferred to the final RWB cross-section. After the peak has passed, the kinetic parameters in the RWB play a larger role in quickly reducing the BOD concentration, because of the ephemeral characteristics of the river (Mannina & Viviani 2010).

Calibration statistics results, in terms of N-S coefficients, are presented in Table 3 for both quantity and quality sub-models and for all simulated events. Some values were not computed because measurements were not available for the specific event and variable. One can see that generally the water quantity processes are better simulated (average efficiency of 0.796) than the quality ones (average efficiency of 0.545). This is mainly due to the greater complexity of water quality processes and the higher uncertainty in measurements (Mannina & Viviani 2010). Negative maximum efficiency values were obtained for some water quality variables, but they were kept because they may be due to measurement errors or specific modelling issues not affecting the general performance of the model.

CONCLUSIONS

The water quality of an ephemeral river was modelled by means of a hydrodynamic water quality model. The model describes water propagation in a river by means of the Saint Venant equations and, for the quality aspects, the 1D advection-dispersion equation. The main water-quality processes that control the state of the Savena river quality have been modelled; these are degradation of dissolved carbonaceous substances, ammonium oxidation, algal uptake and denitrification, dissolved oxygen balance, including depletion by degradation processes and supply by physical reaeration and photosynthetic production. All processes were described assuming 1st order kinetics.

The model was calibrated and evaluated for the Savena River located in Bologna (IT). The results of the evaluation runs showed that the model was generally able to capture the main features of observed values. The discharge, BOD, DO and NH_4 were considered as state variables for the model application. The extent of measurements available, in terms of numbers of samples, was limited. Therefore, further inquiry to other case studies to verify the model is advisable. A sensitivity analysis by means of GLUE methodology enabled us to single out the most sensitive model parameters, which, therefore, should be evaluated carefully. Particularly, the deoxygenation and re-oxygenation constants that, during storm events, are the most important parameters for assessing river water quality state. These considerations are particularly important for the case study shown here, that is, an ephemeral river.

ACKNOWLEDGEMENTS

The authors gratefully acknowledge the contributions of Prof. Sandro Artina and Dr. Marco Maglionico (D.I.S.T.A.R.T.–University of Bologna, Italy) for providing data for the Savena catchment. The authors would like also to thank Eng. Giuseppe Serio for his great help in developing the research.

REFERENCES

van Albada, G. D., van Leer, B. & Roberts, W. W. 1982 A comparative study of computational methods in cosmic gas dynamics. *Astron. Astrophys.* **108**, 76–84.

Downloaded from https://iwaponline.com/wst/article-pdf/446323/288.pdf
by guest

Artina, S., Bardasi, G., Borea, F., Franco, C., Maglionico, M., Paoletti, A. & Sanfilippo, U. 1998 *Water quality modelling in ephemeral streams receiving urban overflows. The pilot study in Bologna*, International Conference: "IMUG–Integrated Modelling User Group", Bruxelles, 21–23 Ottobre 1998.

Artina, S., Bardasi, G., Borea, F., Franco, C., Maglionico, M., Paoletti, A. & Sanfilippo, U. 1999 *Water quality modelling in ephemeral streams receiving urban overflows. The pilot study in Bologna. Proc. 8th International Conference Urban Storm Drainage*, 29/8–3/9, Sydney, Australia, pp. 1589–1596.

Beven, K. J. & Binley, A. M. 1992 The future of distributed models–model calibration and uncertainty prediction. *Hydrol. Process.* **6**(3), 279–298.

Beven, K. J., Smith, P. & Freer, J. 2008 So just why would a modeller choose to be incoherent? *J. Hydrol.* **354**, 15–32.

Brown, L. C. & Barnwell, T. O. 1987 *The Enhanced Stream Water Quality Models QUAL2E and QUAL2E-UNCAS: Documentation and User Manual*. USEPA/6003- 87/007. USEPA, USA.

Chanson, H. 2004 *Environmental Hydraulics of Open Channel Flows*. Elsevier Butterworth-Heinemann, Oxford, UK.

Chapra, S. C. 1997 Surface water–quality modelling. McGraw-Hill Science/Engineering/Math.

Chapra, S. C. & Pelletier, G. J. 2003 *QUAL2K: a Modeling Frame Work for Simulating River and Stream Water Quality: Documentation and Users Manual*. Civil and Environmental Department, Tufts University, Medford, MA.

Cox, B. A. 2003 A review of currently available in-stream water-quality models and their applicability for simulating dissolved oxygen in lowland rivers. *Sci. Total Environ.* **314–316**(1), 335–377.

Fischer, H. B., List, E. J., Koh, R. C. Y., Imberger, J. & Brooks, N. H. 1979 *Mixing in Inland and Coastal Waters*. Academic, San Diego, California.

Freni, G., Mannina, G. & Viviani, G. 2009 Uncertainty assessment of an integrated urban drainage model. *J. Hydrol.* **373**(3–4), 392–404.

Hornberger, G. M. & Spear, R. C. 1981 An approach to the preliminary analysis of environmental systems. *J. Environ. Manage.* **12**, 7–18.

Giusti, E. & Marsili-Libelli, S. 2005 Modelling the interactions between nutrients and the submersed vegetation in the Orbetello Lagoon. *Ecol. Modelling* **184**, 141–161.

Nash, J. E. & Sutcliffe, J. V. 1970 River flow forecasting through conceptual models part I - A discussion of principles. *J. Hydrol.* **10**, 282–290.

Leonard, B. P 1979 A stable and accurate convective modeling procedure based on quadratic upstream interpolation. *Comput. Methods Appl. Mechanics Eng.* **19**, 59–98.

Mannina, G. 2005 Integrated urban drainage modelling with uncertainty for stormwater pollution management, Ph.D. Thesis, Universita' di Catania, Italy.

Mannina, G. & Viviani, G. 2010 A parsimonious dynamic model for river water quality assessment. *Water Sci. Technol.* **61**(3), 607–618.

Marsili-Libelli, S. & Giusti, E. 2008 Water quality modelling for small river basins. *Environ. Modell. Softw.* **23**(4), 451–463.

Molls, T. & Molls, F. 1998 Space-time conservation method applied to Saint Venant equations. *J. Hydraulic Eng. ASCE* **124**(5), 501–508.

Radwan, M., Willems, P., El-sadek, A. & Berlamont, J. 2003 Modelling of dissolved oxygen and biochemical oxygen demand in river water using a detailed and a simplified model. *Proc. int. J. River Basin Manage.* **1**(2), 97–103.

Rauch, W., Henze, M., Koncsos, L., Reichert, P., Shanahan, P., Somlyódy, L. & Vanrolleghem, P. 1998 River water quality modeling: I. State of the art. *Water Sci. Technol.* **38**(11), 237–244.

Reichert, P., Borchardt, D., Henze, M., Rauch, W., Shanahan, P., Somlyody, L. & Vanrolleghem, P. A. 2001 *River Water Quality Model No. 1*. IWA, London.

Ristenpart, E. & Wittenberg, D. 1991 Hydrodynamic water quality simulation–an approximative solution. *Water Sci. Technol.* **24**(6), 157–163.

Streeter, H. W. & Phelps, E. B. 1975 *A study of the pollution and natural purification of the Ohio River. III Factors concerned in the phenomena of oxidation and reaeration*. US Public Health Serv Public Health Bull, 146:75.

Thomann, R. V. & Muller, J. A. 1987 *Principles of Surface Water Quality Modelling and Control*. Harper & Row, New York, p. 644.

Wagenschein, D. & Rode, M. 2008 Modelling the impact of river morphology on nitrogen retention–a case study of the Weisse Elster River (Germany). *Ecol. Model.* **211**, 224–232.

Wang, H. Q. & Lacroix, M. 1997 Optimal weighting in the finite difference solution of the convention-dispersion equation. *J. Hydrol.* **200**, 228–242.

Willems, P. 2000 Probabilistic immission modelling for receiving surface waters. PhD Thesis. Faculty of Engineering. Katholieke Universiteit Leuven. Leuven. Belgium.

Wool, T. A., Ambrose, R. B., Martin, J. L. & Comer, E. A. 2001 *Water Quality Analysis Simulation Program (WASP) Version 6.0 Draft User's Manual*. US Environmental Protection Agency Region 4, Atlanta, GA.

Downloaded from https://iwaponline.com/wst/article-pdf/446323/288.pdf
by guest